Elsevier Editorial System(tm) for Journal of Chromatography A
Manuscript Draft

Manuscript Number:

Title: Ultrafast haplotyping of putative microRNA-binding sites in the WFS1 gene by multiplex PCR and capillary gel electrophoresis

Article Type: MSB 2012

Keywords: WFS1 gene; miRNA-binding site; haplotype; SNP; double-tube allele-specific PCR; capillary gel electrophoresis

Corresponding Author: Professor Andras Guttman,

Corresponding Author's Institution: University of Debrecen

First Author: Marta Kerekgyarto

Order of Authors: Marta Kerekgyarto; Nora Nemeth; Tamas Kerekes; Zsolt Ronai; Andras Guttman

Suggested Reviewers: Julia Khandurina PhD
Senior scientist, Genomatica
jkhandurina@genomatica.com
Genomic expertises

Huba Kalasz PhD
Professor , United Arab Emirates University
huba.huba.kalasz@gmail.com
Separation science

Eva Szoko PhD
Professor , Semmelweis University
eva.szoko@net.sote.hu
Capillary electrophoresis expertises

Opposed Reviewers:

Highlights

- Simultaneous haplotyping of two miRNA-binding sites in the WSF1 is presented.
- A combination allele-specific amplification and capillary electrophoresis was used.
- Ultra-fast size determination of the generated PCR fragments was done by CGE.
- Excellent detection limit of 2 ng/ml was demonstrated.

Ultrafast haplotyping of putative microRNA-binding sites in the WFS1 gene by multiplex PCR and capillary gel electrophoresis

Márta Kerékgyártó[a], Nóra Németh[b], Tamás Kerekes[c], Zsolt Rónai[b] and András Guttman[a*]

[a]*Horváth Laboratory of Bioseparation Sciences, University of Debrecen, H-4032 Debrecen, Nagyerdei krt. 98, Hungary;* [b]*Department of Medical Chemistry, Semmelweis University, H-1094 Budapest, Tuzolto u. 37-47, Hungary;* [c]*Centre for Clinical Genomics and Personalized Medicine, Medical and Health Science Center, University of Debrecen, H-4032 Debrecen, Nagyerdei krt. 98, Hungary*

[*] To whom correspondence should be addressed: Phone: +36(52) 414-717/64182; Fax: +36 (52) 414-717/55539; E-mail: guttman.andras@hlbs.org

ABSTRACT

The transmembrane protein wolframin (WSF1) plays a crucial role in cell integrity in pancreatic beta cells and maintaining ER homeostasis. Genetic variations in the WFS1 gene have been described to be associated with Wolfram syndrome or type 2 diabetes mellitus. In this paper we report on an efficient double-tube allele-specific amplification method in conjunction with ultrafast capillary gel electrophoresis for direct haplotyping analysis of the SNPs in two important miRNA-binding sites (*rs1046322* and *rs9457*) in the WFS1 gene. An automated single-channel capillary gel electrophoresis system was utilized in the method that provided dsDNA fragment analysis in less than 240 sec. The light-emitting diode induced fluorescence (LEDIF) detection system enabled excellent sensitivity for automated haplotyping of a large number of clinical samples. The detection limit was 0.002 ng/µL using field amplified injection from water diluted samples. The dynamic quantitation range was 0.08 - 10.00 ng/µL (R^2=0.9997) in buffer diluted samples.

Keywords: WFS1 gene; miRNA-binding site; haplotype; SNP; double-tube allele-specific PCR; capillary gel electrophoresis

1. Introduction

Wolframin (WFS1) is a transmembrane protein in the endoplasmic reticulum (ER), which is produced at higher levels in pancreatic beta cells and specific neurons in the central nervous system [1]. It plays an important role in the ER calcium homeostasis [1-3] and in the ER stress response [4]. As an ER stress signaling suppressor it affects the negative regulatory feedback loop of the ER stress signaling network [5], which is strictly controlled in pancreatic beta cells to produce adequate amounts of insulin in case of blood glucose levels fluctuation [6,7]. Moreover

it plays an essential role in the cell integrity of pancreatic beta cells and maintains ER homeostasis [8]. When the wolframin gene (WFS1) is inactivated in beta cells of rodents it causes ER stress and death of the beta cells by accelerated apoptosis [9]. Mutations in the WFS1 gene are causing the so called Wolfram syndrome [10], which includes young onset non-autoimmune insulin dependent diabetes mellitus, diabetes insipidus, optic atrophy, deafness or other neurological and endocrine abnormalities [11,12]. An increased prevalence of diabetes mellitus in reference to Wolfram syndrome was reported in first-degree relatives of patients [13], suggesting a probable effect of WSF1 mutation heterozygosis. The occurrence of single nucleotide polymorphisms (SNPs) in WFS1 has recently been demonstrated to be associated with type 2 diabetes mellitus in populations of European descents [14-16].

MicroRNAs are non-coding short ribonucleic acids, which are responsible for the translation regulation of gene expression. The homeostatic protein level is modified due to the interaction between miRNAs and its targets, resulting in possible phenotype changes, such as disease. This modified interaction can be caused by SNPs either in the gene of the miRNA or its target. SNPs are rare in miRNA-coding genes [17] and referred to as miRSNPs. They were shown to be associated with different illnesses, such as various types of cancers [18], autoimmune diseases [19], or neurological disorders [20].

Multiplex PCR techniques gained recent popularity in assessing genetic variation by simultaneous analysis of two or more DNA regions or genetic variations of interest [21,22]. Development of a multiplex PCR reaction involves the design of the relevant primer sets and examination of their various combinations, different reaction components and/or thermal cycling conditions. Multiplexing in this way increases the throughput of the amplification steps especially when capillary gel electrophoresis is utilized with rapid separation and quantitation capability for the analysis of the resulting fragments [23]. Multiplexing on the other hand may lead to unequal amplification, particularly at the larger DNA fragment range, so the above mentioned reaction design is of high importance [24].

Simultaneous study of multiple polymorphisms, such as haplotyping, is getting more and more attention to analyze the genetic background of complex diseases [25]. Haplotype, the relative chromosomal localization of the alleles of the polymorphic loci, can serve as very effective genetic markers [26]. Haplotype identification can be accomplished by several ways. One of the oldest methods is based on the theory of Mendelian inheritance of families or larger pedigrees; however, this approach has several drawbacks [27,28]. Other methods, such as computer-based haplotype prediction can also be suitable for haplotypes determination, but haplotypes of individual samples cannot be obtained by this approach [28,29]. Direct haplotype determination by allele-specific amplification (ASA), also referred to as molecular haplotyping, is one of the most efficient and reliable methods that is based on appropriate amplification providing the required haplotype information without the need of biological parents' genotype information [30]. Moreover this technique provides fast and reliable genotyping data of any SNP in a single

tube polymerase chain reaction (mPCR) followed by electrophoresis analysis [31,32]. This amplification method is based on the use of an allele-specific primer as its 3'-end hybridizes to the SNP site. This is followed by amplification using a DNA-polymerase enzyme, which is lacking 3'-exonuclease activity, thus, amplification can only be carried out in the case the primer completely matches with the template. The technique when two allele-specific primers are used for convenient allelic variant determination in two separate reactions is referred to as double-tube specific-allele amplification [33]. This novel haplotyping technique was introduced earlier to investigate the -616CG and -521CT SNPs in the Dopamine D4 Receptor gene by Szantai et al [24]. The resulting DNA fragments after the amplification process are regularly analyzed by conventional agarose/polyacrylamide slab gel electrophoresis for genotype or haplotype determination. However, these methods are labor intensive and time consuming, also requiring improvements in terms of resolving power and analysis throughput. Recent developments in the field of capillary gel electrophoresis resulted in rapid electrophoresis-based fragment analysis techniques that can readily speed up this process. In addition to its speed, capillary gel electrophoresis offers further advantages over traditional slab gel electrophoresis, such as low reagent consumption, small sample volume requirement and the option of multiplexing [30]. CGE combined with light-emitting diode induced fluorescence (LEDIF) detection enables sensitive detection of dsDNA fragments and can be readily applied for automated large scale analyses in clinical settings [34].

In this paper we report on haplotyping (i.e., simultaneous multiple genotyping) of two adjacent putative miRNA-binding SNPs in the WFS1 gene by combining double-tube allele-specific amplification and rapid capillary gel electrophoresis with LED-induced fluorescent detection to analyze the resulting DNA fragments. The detection limit of the method was as low as 0.002 ng/µL using field amplified injection method.

2. Materials and Methods

2.1. Chemicals

The HotStar *Taq* DNA polymerase including the 10× reaction buffer and the Q-solution was used from Qiagen (Valencia, CA, USA) for the allele-specific PCR reaction. The oligonucleotide primers were obtained from Sigma Genosys (Woodlands, TX, USA). For agarose slab gel electrophoresis, the 100 base pair DNA ladder (GeneRuler, Thermo Fisher Scientific, FL, USA) was diluted to a final concentration of 0.5 µg/µL and stored at –20 °C. In CGE separations, the Qsep100 DNA-CE high-resolution gel buffer and Qsep100 DNA-CE running buffer were used (BiOptic, New Taipei City, Taiwan). The DNA alignment marker (20 base pair, 1.442 ng/µL and 5000 base pair, 1.852 ng/µL) and the DNA size marker (50–3000 bases, 10.5 ng/µL) were from BiOptic and stored at –20 °C. The WFS1 PCR samples (576 bp, 253.19 ng/µL) were diluted to the appropriate concentrations with MilliQ-grade water (Millipore, Billerica, MA, USA) or dilution buffer (BiOptic) for the detection limit and linearity studies and stored at –20 °C.

2.2. Non-invasive DNA sampling and DNA extraction

DNA samples were obtained using non-invasive DNA sampling (buccal swabs) from healthy Hungarian volunteers. The study protocol was approved by the Scientific and Research Ethics Committee of the Medical Research Council of Hungary (ETT TUKEB). DNA samples were purified by standard procedure as described earlier [35,36].

2.3. Molecular haplotype analysis

Direct haplotype determination of the *rs1046322* and *rs9457* SNPs was carried out by allele-specific amplification. The HotStarTaq polymerase kit (Qiagen) was used for the PCR amplification and each DNA sample was analyzed in two separate reactions. Both reaction mixtures contained approximately 4 ng gDNA template, 200 µM deoxyadenosine triphosphate (dATP), deoxycitidine triphosphate (dCTP), deoxyguanosine triphosphate (dGTP) and deoxythymidine triphosphate (dTTP), 0.5 U HotStar *Taq* DNA polymerase with 1× reaction buffer and 1× Q-solution, as well as 1 µM of each outer primer (sense: 5' TCT GTC CAC TCT GAA TAC 3' and antisense: 5' CAG GCT CTT CTA AAC ACT 3'). Reaction mixture-I was used to analyze the presence of the *rs1046322A* and *rs9457C* alleles, as well as their haplotype, thus it contained the *rs1046322A* specific sense (5' GAG CCT GAC CTT TCT GAA 3') and the *rs9457C* specific antisense (5' CCA CTA CCT GCT GGA G 3') primers. Reaction mixture-II was employed to investigate the other possible variants (*rs1046322G*-specific sense primer: 5' GAG CCT GAC CTT TCT GAG 3', *rs9457G*-specific antisense primer: 5' CCA CTA CCT GCT GGA C 3'). PCR amplification reactions were carried out in a total volume of 10 µL. The primers were tested by the Oligo 5.0 software (Molecular Biology Insides, Cascade, CO, USA). Thermocycling was initiated at 95 °C for 15 min, this step also served for the activation of the hot-start DNA polymerase. It was followed by 40 cycles of denaturation at 94 °C for 30 s, annealing at 55 °C for 30 s and then extension at 72 °C for 1 min. The last step of the amplification was a final extension at 72 °C for 10 min after that the PCR products were kept at 8 °C.

For the detection limit and linearity studies, the PCR reaction mixture contained approximately 4 ng gDNA template, 200 µM of each deoxyribonucleotide triphosphate (dATP, dCTP, dGTP and dTTP), 0.05 U/µL HotStar *Taq* DNA polymerase with 1× reaction buffer and 1× Q-solution, as well as 1 µM of each primer (sense: 5' GCC CTT CTC GAG TCT TGC AGC GCC GGA ATA GGC 3' and antisense: 5' GCA GAA GCT TAA GTT GTT CGG GAG CAG CTG AAC G 3'). The amplification reaction was carried out in a total volume of 100 µL. The first step was the initial denaturation of the gDNA at 95 °C for 15 min; it was followed by 40 cycles of denaturation (94 °C, 30 sec), annealing (65 °C, 30 sec) and then extension (72 °C, 1 min). The last step of the PCR was a final extension at 72 °C for 10 min after that the sample was kept at 8 °C.

2.4. PCR- fragment analysis by agarose slab gel electrophoresis

The PCR products were first analyzed by agarose slab gel electrophoresis. Agarose powder (final concentration: 2% w/v) was mixed with electrophoresis buffer (1× TAE buffer; 40 mM Tris, 20 mM acetic acid, and 1 mM EDTA, pH 8.0) and heated until the agarose completely dissolved. Ethidium bromide was added to the melted gel in a final concentration of 0.5 µg/mL. After solidification at room temperature, 20 ng of PCR products and the 100 bp DNA sizing ladder (100–1000 bp, 0.5 µg/uL) containing DNA loading Dye (6× loading Dye: 10 mM Tris-HCl (pH 7.6), 0.03% bromophenol blue, 0.03% xylene cyanol FF, 60% glycerol and 60 mM EDTA) were loaded into the sample wells followed by electrophoresis (100 V for 45 min, BioRad PowerPac 300; Hercules, CA, USA). The separated DNA bands were visualized in a UV light box (Bio Rad Gel-Doc XR System).

2.5 PCR- fragment analysis by capillary gel electrophoresis

Rapid capillary gel electrophoresis analysis of the PCR-products were accomplished in a single-channel capillary cartridge Qsep100 DNA-CE unit (BiOptic) with an 11 cm effective length (total length: 15 cm) fused silica capillary (internal diameter: 75 µm). The capillary was washed with 5 mL of 70 °C MilliQ-grade water (Millipore) for 500 s before the first use. Then 5 mL of Qsep100 DNA-CE high-resolution gel buffer was transferred into the gel reservoir and the capillary was purged twice for 1000 s. The gel-buffer system contained ethidium-bromide to accommodate fluorescent detection. Prior to each injection the sieving matrix was replaced in the capillary by means of a 10 s purge step, followed by injection of the DNA alignment marker (4 kV for 10 s). After that the separation capillary was immersed into MilliQ-grade water (0 kV for 1 sec) as a washing step to avoid any sample cross-contamination. The samples (as well as the DNA size marker and/or PCR-products) were introduced electrokinetically from a 96-well plate (4 kV for 10 s). Separations were carried out at ambient temperature by applying 6 kV electric potential. Data analysis was performed using the Q-Expert software package (BiOptic). All buffers and reagents were filtered through 0.22 µm pore size Acrodisc syringe filters (Millipore, Billerica, MA, USA) and degassed prior to use. Other reagents and chemicals for sample preparation were purchased from Sigma-Aldrich (St. Louis, MO, USA).

3. Results and Discussion

3.1. Direct haplotype determination by allele-specific PCR

Haplotype determination of adjacent polymorphic loci is of high importance, especially in case of SNPs with biological significance. The *rs9457* and *rs1046322* SNPs, located in the WFS1 gene 3’ UTR, are assumable miR-SNPs and their *in silico* data analysis suggested that they may alter the binding of miR-185 and miR-668, respectively. Consequently in case of double heterozygote samples (*rs1046322AG* and *rs9457CG*) haplotype determination is essential, since otherwise it is uncertain if the two allelic variants possibly affecting miRNA-binding are located on the same mRNA (“cis”) or can be found on two different chromosomes (“trans”) as delineated in Figure 1.

An allele-specific PCR based approach was elaborated for the haplotype determination of the two SNPs of interest. The principle of the technique was the simultaneous application of two outer and two allele-specific primers in a multiplex PCR reaction as shown in Figure 2. The allele-specific primers were designed to anneal to the SNP by their 3' end. Based on chromosomal localization, a sense *rs1046322*- and antisense *rs9457*-specific primer were applied in the reaction. One reaction mixture tested the presence of one allele at each loci as well as one haplotype combination, consequently two reaction mixtures were required for genotype and haplotype determination, whereas further two can be applied for conformation (Figure 2). Panel A in Figure 2 depicts the analysis using reaction mixture-I containing the sense *rs1046322A*- and the antisense *rs9457C*-specific primers. In case of the presence of an A allele at the *rs1046322* site, a 488-bp-long fragment was generated by the *rs1046322A*-specific and the antisense outer primers. Similarly if the sample possessed the C allele at the *rs9457* locus, the primer specific for this variant together with the sense outer primer could amplify a 437-bp-long fragment. More importantly, if the *rs1046322A* and *rs9457C* alleles are located on the same chromosome, a 384-bp-long product could also be observed as this product is generated by the two allele-specific primers and suggested the presence of the A–C haplotype. The longest, 541-bp outer fragment is a control product synthesized independently of the genotype and haplotype of the sample of interest.

Reaction mixture-II worked similarly; however, it contained the *rs1046322G*- and *rs9457G*-specific primers in combination with the outer oligos as shown Figure 2 Panel B. Thus, a 488-bp-long product could be observed in case of the *rs1046322G* allele, a 437-bp-long product produced if the *rs9457G* allele was present, whereas the 384-bp-long product suggested the G–G haplotype. Genotype and haplotype information could be unambiguously determined by these two reactions. For additional validation, two redundant combinations were also applied in a subset of 24 samples (i.e. *rs1046322G* allele-, *rs9457C* allele- and thus G–C haplotype specific reaction and *rs1046322A* allele-, *rs9457G* allele- and consequently A–G haplotype specific mixture). Results of these analyses confirmed the data obtained by the original setup. Then 95 healthy Hungarian individuals were analyzed by the described method and the obtained results were in 98.9% concordance with the genotype data determined earlier by an independent approach employing sequence specific TaqMan probes (data not shown). The single discordant result could be resolved by a repeated genotype and haplotype determination.

Figure 2 Panel C shows the conventional agarose slab gel electrophoresis based genotype and haplotype determination of the *rs9457* and *rs1046322* SNPs in case of double heterozygote samples. The 100 bp DNA sizing marker (M) was used with the PCR samples (1 and 2) to assess the size of the double allele-specific amplicons in the case of both haplotypes verification. One of the haplotype (*rs104632A-rs9457C*) was labeled with A and the other (*rs104632G-rs9457G*) was indicated with B in Figure 2 Panel C.

3.2. Haplotype determination by capillary gel electrophoresis

The final step of the haplotyping protocol was capillary gel electrophoresis based size determination of the dsDNA fragments from the multiplex amplification reaction. Figure 3 depicts the capillary gel electrophoresis traces of the PCR fragments generated during haplotype determination. A DNA sizing ladder in the range of 50–3000 bp was used for fragment size assessment in a final concentration of 10.5 ng/µL (upper trace). The analysis of the mPCR samples is shown in the middle and lower traces. The samples were coinjected with the lower and upper alignment markers (M_1: 20 bp dsDNA and M_2: 5000 bp dsDNA) to attain high fragment sizing accuracy. The middle trace in Figure 3 shows the separation of three dsDNA fragments from the multiplex amplification reaction mixture-1 with calculated sizes of 454, 500 and 583 bp fragments, corresponding to 437, 488 and 541 bp of the actual PCR reactions (see variance data in Table 1). The lower trace in Figure 3 depicts the separation of four dsDNA fragments from amplification reaction mixture-2 with calculated sizes of 399, 457, 504 and 591 bp fragments (corresponding to the actual fragment sizes of 384, 437, 488 and 541 bp with better than 95% average accuracy) by the rapid CE-LEDIF based method (see variance data in Table 1). In Table 1 the size (bp) of each multiplex PCR sample was calculated by Q-Expert software package (BiOptic) with the accuracy range of 2.4–9.2%. Furthermore the concentration of each DNA fragment was calculated based on their peak areas as listed in Table 1.

3.3. Limit of detection (LOD) and detector linearity

Figure 4, Panel A compares the resulting signal from the electropherograms after the injection of different concentration samples from 0.01 ng/ µL to as low as 0.002 ng/µL, this latter being the detection limit. In this instance the dilution of the 576 bp DNA fragment was done in water. When the detector linearity experiments were conducted with the same water diluted samples, the linear detection range was quite narrow (1.5 orders of magnitude) due to the effect of field amplification. Detection linearity was therefore determined by using a dilution series in sample buffer (BiOptic) in which case a linear detector response was obtained in a large interval of 0.08 ng/µL to 10.0 ng/ µL with an R^2 = 0.9997, as shown in Figure 4, Panel B and in Table 2. Again, we would like to emphasize that injection from water diluted samples results in much larger sample intake as the buffer co-ions do not compete with the sample molecules, resulting in excellent LOD. Sample concentration measurement on the other hand was more precise from buffer diluted samples as shown in Table 1.

4. Conclusions

Capillary gel electrophoresis is an automated, high-throughput DNA fragment analysis method that can be readily applied for the investigation of a large number of samples. In this paper we introduced a rapid CE-LEDIF based method in conjunction with multiplex PCR amplification for genotyping and haplotyping of two important, adjacent miRNA-binding sites (*rs1046322* and *rs9457*) in the WSF1 gene. The separation performance of the system was demonstrated by ultrafast (<240 sec) and accurate (2.4–9.2%) sizing analysis of multiplex PCR samples, also exhibiting excellent detector linearity (R^2=0.9997) from 0.08–10.0 ng/µL concentration. The

LOD of the system was 0.08 ng/µL for samples in dilution buffer and 0.002 ng/µL for samples in water. In summary, this CGE-LEDIF system is a sensitive and easy to use bio-analytical tool for automated haplotyping of a large number of clinical samples.

5. Acknowledgements

This project was supported by the Hungarian Grant OTKA grants of K81839 and K83766 as well as the János Bolyai Research Scholarship (BO/00089/10/5) of the Hungarian Academy of Sciences. Provision of the capillary gel electrophoresis system by BiOptic, Inc. is also greatly appreciated. The authors have declared no conflicts of interest.

6. References

[1] K. Takeda, H. Inoue, Y. Tanizawa, Y. Matsuzaki, J. Oba, Y. Watanabe, K. Shinoda, Y. Oka, Hum Mol Genet 10 (2001) 477.
[2] A.A. Osman, M. Saito, C. Makepeace, M.A. Permutt, P. Schlesinger, M. Mueckler, Journal of Biological Chemistry 278 (2003) 52755.
[3] D. Takei, H. Ishihara, S. Yamaguchi, T. Yamada, A. Tamura, H. Katagiri, Y. Maruyama, Y. Oka, Febs Letters 580 (2006) 5635.
[4] S.G. Fonseca, M. Fukuma, K.L. Lipson, L.X. Nguyen, J.R. Allen, Y. Oka, F. Urano, Journal of Biological Chemistry 280 (2005) 39609.
[5] S.G. Fonseca, S. Ishigaki, C.M. Oslowski, S. Lu, K.L. Lipson, R. Ghosh, E. Hayashi, H. Ishihara, Y. Oka, M.A. Permutt, F. Urano, J Clin Invest 120 (2010) 744.
[6] S.G. Fonseca, K.L. Lipson, F. Urano, Antioxid Redox Signal 9 (2007) 2335.
[7] K.L. Lipson, S.G. Fonseca, S. Ishigaki, L.X. Nguyen, E. Foss, R. Bortell, A.A. Rossini, F. Urano, Cell Metab 4 (2006) 245.
[8] N. Cheurfa, G.M. Brenner, A.F. Reis, D. Dubois-Laforgue, R. Roussel, J. Tichet, O. Lantieri, B. Balkau, F. Fumeron, J. Timsit, M. Marre, G. Velho, Diabetologia 54 (2011) 554.
[9] A.C. Riggs, E. Bernal-Mizrachi, M. Ohsugi, J. Wasson, S. Fatrai, C. Welling, J. Murray, R.E. Schmidt, P.L. Herrera, M.A. Permutt, Diabetologia 48 (2005) 2313.
[10] D.J. Wolfram, H.P. Wagener, Mayo Clinic Proceedings (1938) 715.
[11] T.G. Barrett, S.E. Bundey, A.F. Macleod, Lancet 346 (1995) 1458.
[12] L. Rigoli, F. Lombardo, C. Di Bella, Clin Genet 79 (2011) 103.
[13] F.C. Fraser, T. Gunn, J Med Genet 14 (1977) 190.
[14] P.W. Franks, O. Rolandsson, S.L. Debenham, K.A. Fawcett, F. Payne, C. Dina, P. Froguel, K.L. Mohlke, C. Willer, T. Olsson, N.J. Wareham, G. Hallmans, I. Barroso, M.S. Sandhu, Diabetologia 51 (2008) 458.
[15] V. Lyssenko, A. Jonsson, P. Almgren, N. Pulizzi, B. Isomaa, T. Tuomi, G. Berglund, D. Altshuler, P. Nilsson, L. Groop, New England Journal of Medicine 359 (2008) 2220.
[16] M.S. Sandhu, M.N. Weedon, K.A. Fawcett, J. Wasson, S.L. Debenham, A. Daly, H. Lango, T.M. Frayling, R.J. Neumann, R. Sherva, I. Blech, P.D. Pharoah, C.N. Palmer, C. Kimber, R. Tavendale, A.D. Morris, M.I. McCarthy, M. Walker, G. Hitman, B. Glaser, M.A. Permutt, A.T. Hattersley, N.J. Wareham, I. Barroso, Nature Genetics 39 (2007) 951.
[17] M.A. Saunders, H. Liang, W.H. Li, Proceedings of the National Academy of Sciences of the United States of America 104 (2007) 3300.

[18] L.J. Chin, E. Ratner, S.G. Leng, R.H. Zhai, S. Nallur, I. Babar, R.U. Muller, E. Straka, L. Su, E.A. Burki, R.E. Crowell, R. Patel, T. Kulkarni, R. Homer, D. Zelterman, K.K. Kidd, Y. Zhu, D.C. Christiani, S.A. Belinsky, F.J. Slack, J.B. Weidhaas, Cancer Research 68 (2008) 8535.
[19] S. Tan, J.M. Guo, Q.L. Huang, X.P. Chen, J. Li-Ling, Q.W. Li, F. Ma, Febs Letters 581 (2007) 1081.
[20] K.P. Jensen, J. Covault, T.S. Conner, H. Tennen, H.R. Kranzler, H.M. Furneaux, Molecular Psychiatry 14 (2009) 381.
[21] M.C. Edwards, R.A. Gibbs, PCR Methods Appl 3 (1994) S65.
[22] C.P. Kimpton, P. Gill, A. Walton, A. Urquhart, E.S. Millican, M. Adams, PCR Methods Appl 3 (1993) 13.
[23] J.M. Butler, C.M. Ruitberg, P.M. Vallone, Fresenius Journal of Analytical Chemistry 369 (2001) 200.
[24] E. Szantai, A. Szilagyi, A. Guttman, M. Sasvari-Szekely, Z. Ronai, J Chromatogr A 1053 (2004) 241.
[25] B. Lewin, Genes VI, Oxford University Press, Oxford ; New York, 1997.
[26] E. Szantai, Z. Ronai, M. Sasvari-Szekely, A. Guttman, Anal Biochem 352 (2006) 148.
[27] C.L. Barr, Y. Feng, K.G. Wigg, R. Schachar, R. Tannock, W. Roberts, M. Malone, J.L. Kennedy, Am J Med Genet 105 (2001) 84.
[28] S.E. Hodge, M. Boehnke, M.A. Spence, Nature Genetics 21 (1999) 360.
[29] L. Excoffier, M. Slatkin, Molecular Biology and Evolution 12 (1995) 921.
[30] E. Szantai, Z. Ronai, A. Szilagyi, M. Sasvari-Szekely, A. Guttman, J Chromatogr A 1079 (2005) 41.
[31] Z. Ronai, C. Barta, A. Guttman, K. Lakatos, J. Gervai, M. Staub, M. Sasvari-Szekely, Electrophoresis 22 (2001) 1102.
[32] Z. Ronai, E. Szantai, R. Szmola, Z. Nemoda, A. Szekely, J. Gervai, A. Guttman, M. Sasvari-Szekely, American Journal of Medical Genetics Part B-Neuropsychiatric Genetics 126B (2004) 74.
[33] E. Szantai, A. Guttman, Electrophoresis 27 (2006) 4896.
[34] M. Kerekgyarto, T. Kerekes, E. Tsai, V.D. Amirkhanian, A. Guttman, Electrophoresis 33 (2012) 2752.
[35] Z. Ronai, A. Guttman, Z. Nemoda, M. Staub, H. Kalasz, M. Sasvari-Szekely, Electrophoresis 21 (2000) 2058.
[36] M. Sasvari-Szekely, A. Gerstner, Z. Ronai, M. Staub, A. Guttman, Electrophoresis 21 (2000) 816.

Figure Captions

Figure 1. Schematic representation of the putative effect of the two SNPs on miRNA binding. Genotypes and haplotypes can be determined by allele-specific amplification using sense *rs1046322*- and antisense *rs9457*-specific primers in different combination in case of double heterozygote samples (Sample 1 and Sample 2). The four thick gray lines indicate the four haplotypes on the same chromosomes: A–C, G–G, A–G and G–C.

Figure 2. Allele-specific multiplex PCR-based direct haplotype determination of the *rs1046322* and *rs9457* SNPs in the WSF1 gene. (A) Fragments expected in the presence of the sense *rs1046322A*- and the antisense *rs9457C*-specific primers in combination with the outer oligos. The 384-bp-long fragment was generated by *rs1046322A* and *rs9457C* primers and demonstrated the presence of the A–C haplotype. **(B)** PCR products obtained in the presence of the *rs1046322G*- and *rs9457G*-specific primers in combination with the outer oligos. The 384-bp-long product demonstrated the presence of the G–G haplotype. **(C)** Genotype and haplotype readings by agarose slab gel electrophoresis. M: 100 base pair DNA sizing marker; Lanes 1-2: PCR samples: *A:* 437, 488, 541 bp dsDNA fragments; *B:* 384, 437, 488, 541 bp dsDNA fragments from the multiplex amplification reaction. Separation conditions: 2% agarose gel in 1 × TAE containing 0.5 µg/mL ethidium bromide; U=100V; t=45 min; room temperature.

Figure 3. Capillary gel electrophoresis based fragment analysis of representative multiplex PCR amplicons. Upper trace: DNA sizing ladder (M: 50 to 3000 bp) co-injected with the lower (M1 = 20 bp) and upper (M2 = 5000 bp) alignment markers; Middle and lower traces: representative PCR fragments of 1 and 2 were the same as in Figure 2, respectively, with the respective alignment markers. Separation conditions: marker and sample injection: 4kV/10sec; separation voltage 6 kV; capillary: 75-µm i.d., total length of 15 cm length (effective separation length: 11 cm); ambient temperature.

Figure 4. LOD and detection linearity measurements. (A) Determination of the limit of detection (LOD) with a representative PCR fragment (576 bp) serially diluted in water compared to the sizing ladder. **(B)** Detection linearity study using the of the 576 bp PCR fragment serially diluted in the sample buffer. Separation conditions, sizing ladder and lower and upper alignment markers were the same as in Figure 3.

Figure 1

Click here to download high resolution image

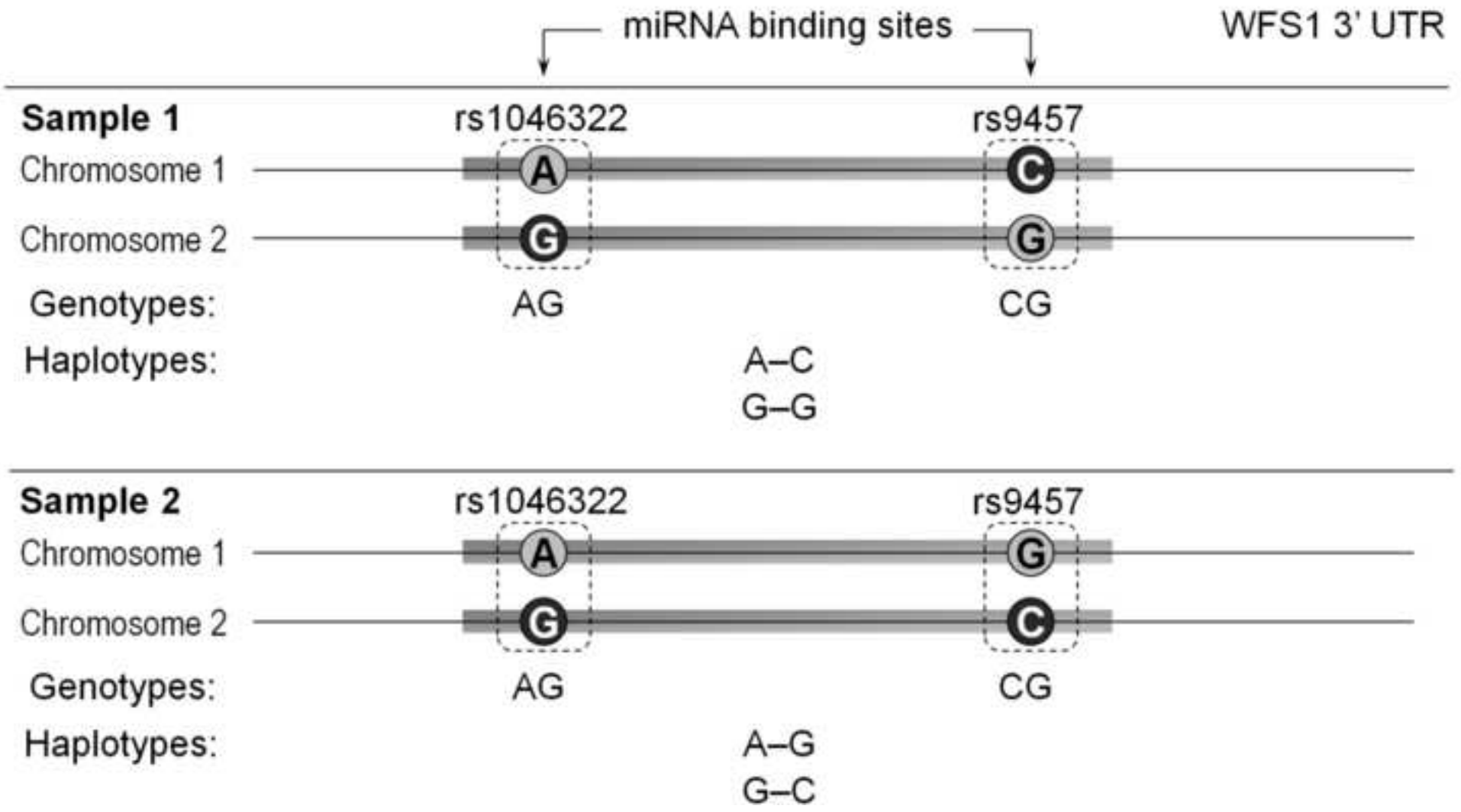

Figure 2A

Click here to download high resolution image

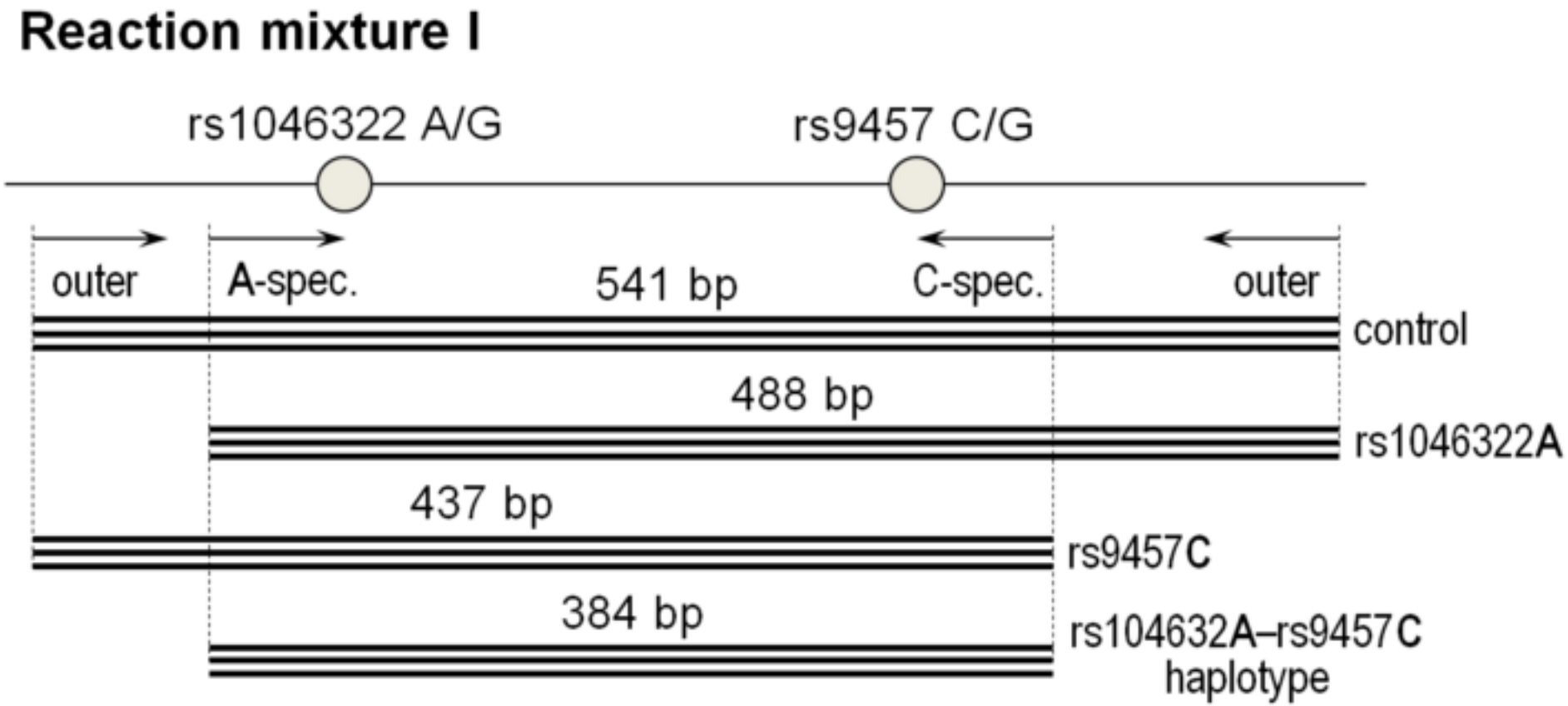

Figure 2B

Click here to download high resolution image

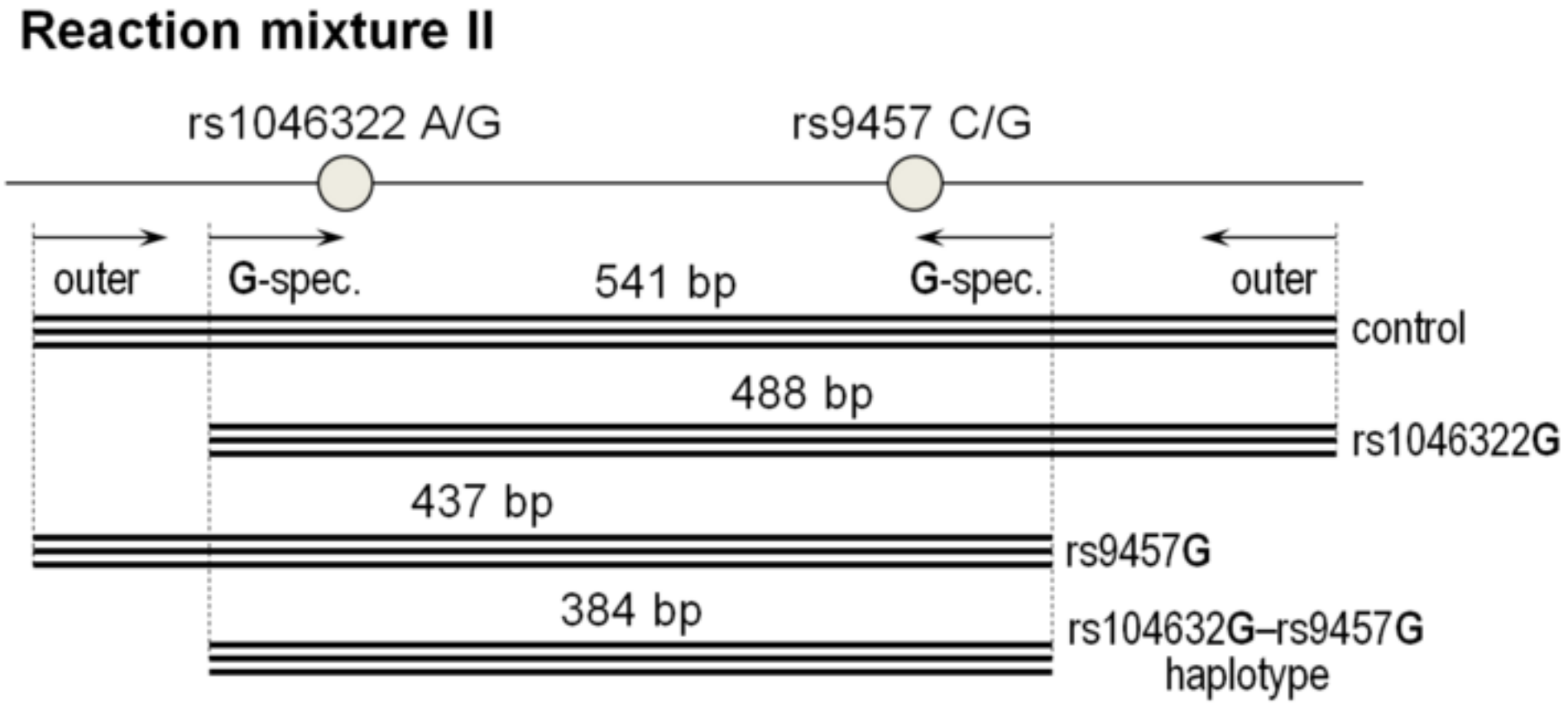

Figure 2C

Click here to download high resolution image

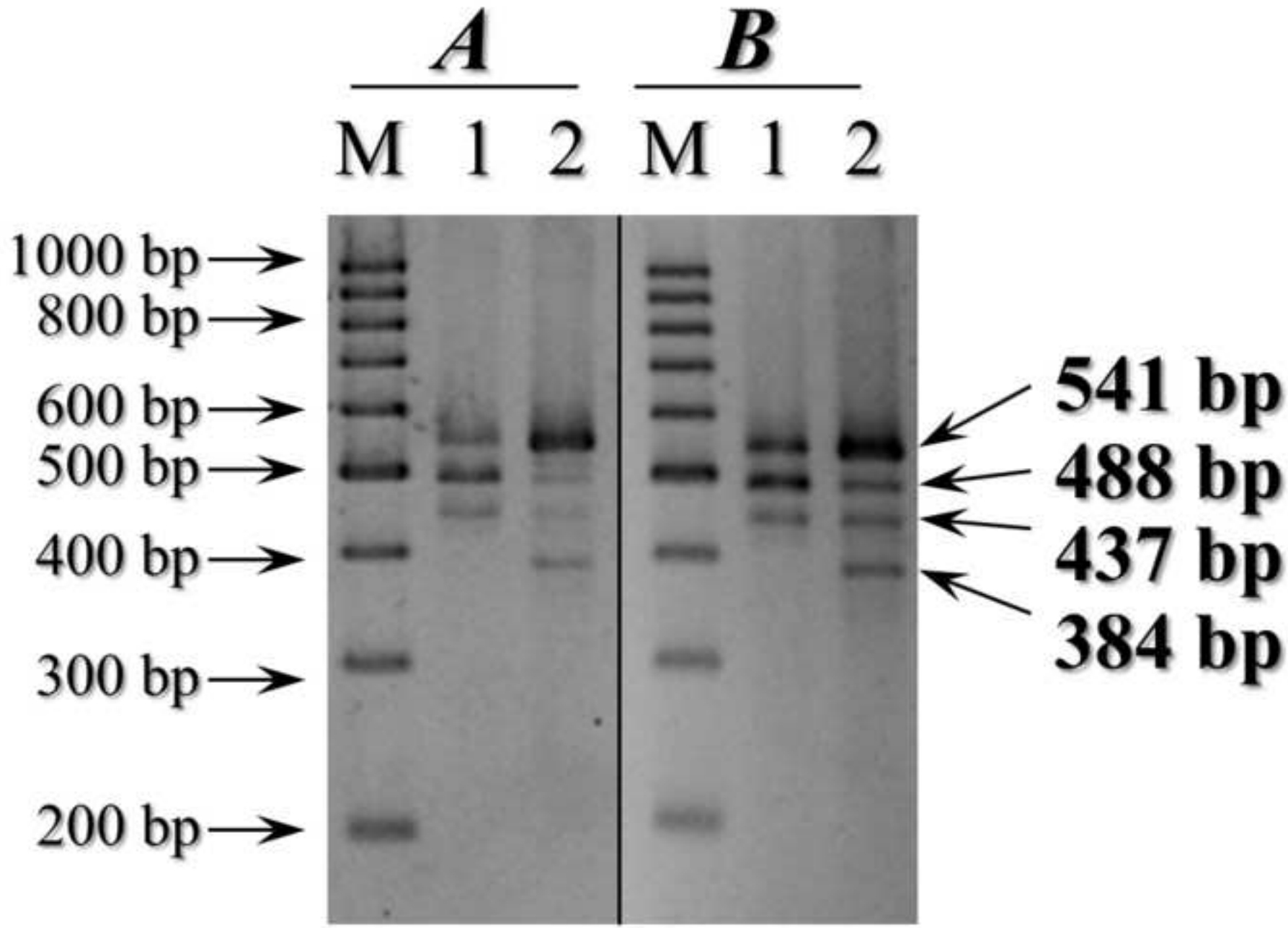

Figure 3

Click here to download high resolution image

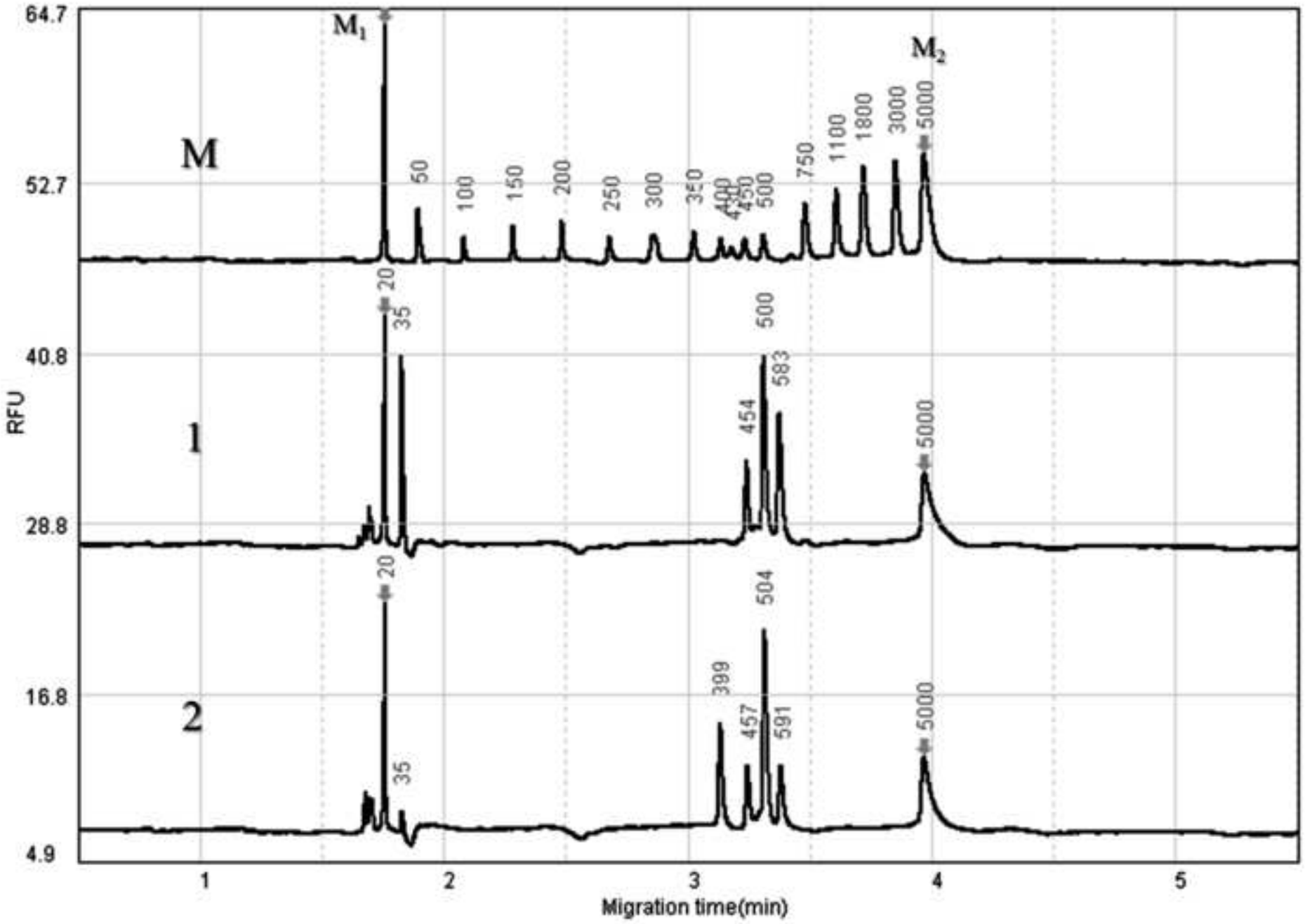

Figure 4A

Click here to download high resolution image

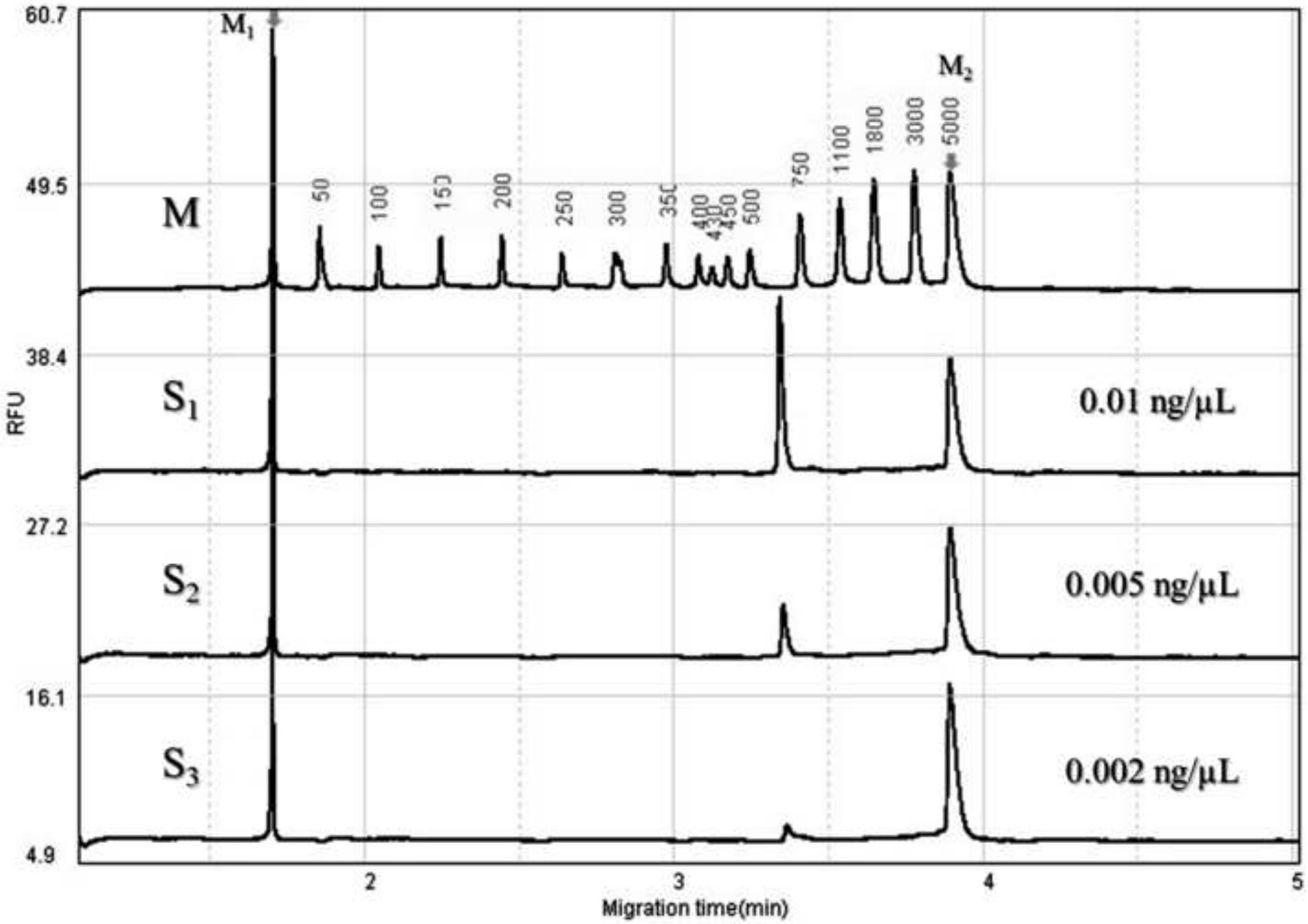

Figure 4B

Click here to download high resolution image

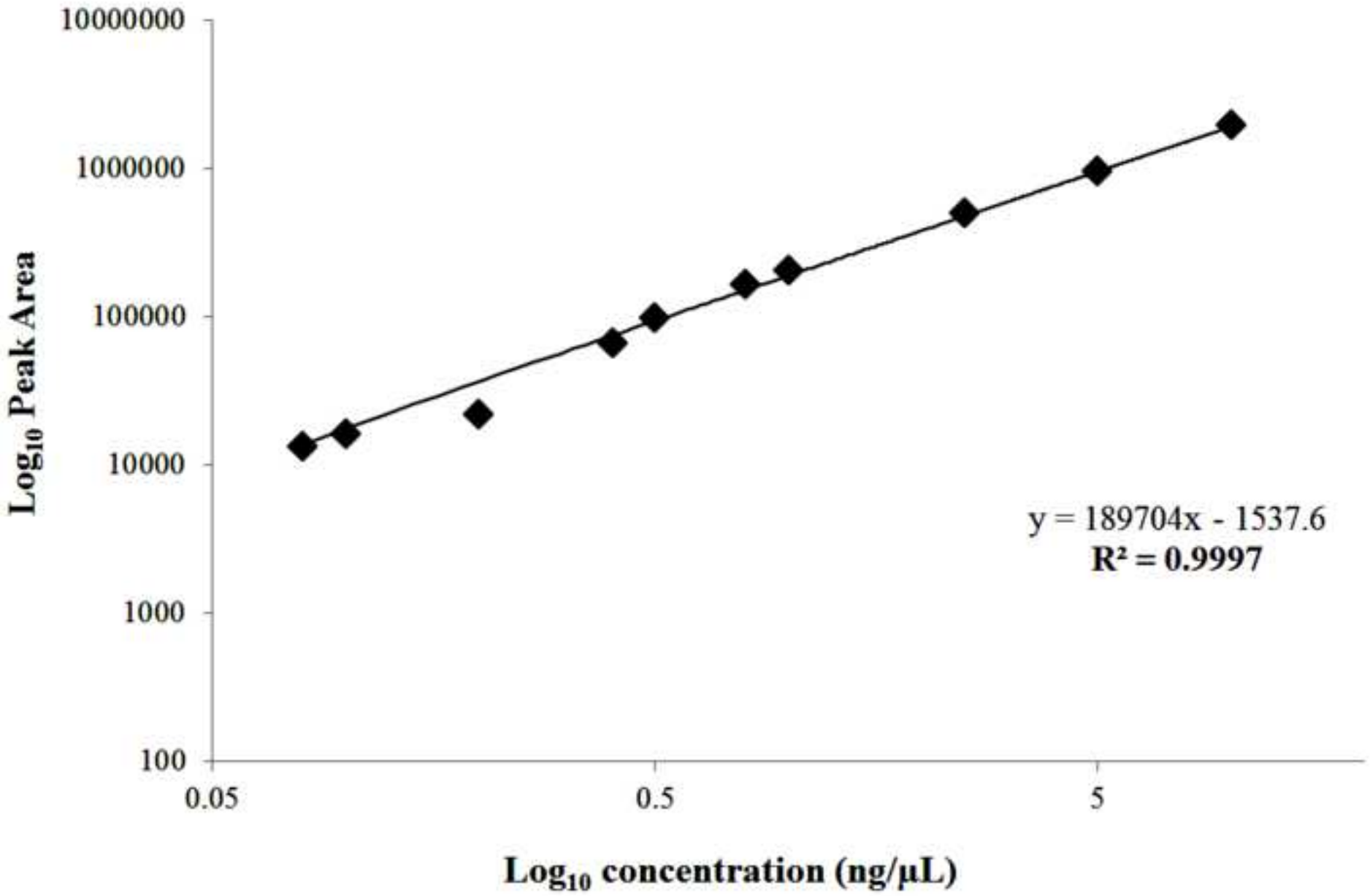

TABLES

Table 1. Base pair accuracy determination and calculated concentrations of the multiplex PCR samples using CGE.

1. PCR sample (Figure 3 middle trace)					2. PCR sample (Figure 3 lower trace)				
Fragment (bp)	**Measured** (bp)	**Variance** (bp)	**Accuracy** (%)	**Concentration** (µg/µL)	**Fragment** (bp)	**Measured** (bp)	**Variance** (bp)	**Accuracy** (%)	**Concentration** (µg/µL)
-	-	-	-	-	**384**	399	15	3.9	1.65
437	454	17	3.8	1.34	**437**	457	20	4.5	0.90
488	500	12	2.4	4.16	**488**	504	16	3.2	4.04
541	583	42	7.7	2.38	**541**	591	50	9.2	1.09

Table 2. CGE Detector linearity of measured by injecting the 576 bp PCR sample in the 10.00-0.08 ng/µL concentration range.

Detector linearity of the representative PCR sample										
	No 1.	**No 2.**	**No 3.**	**No 4.**	**No 5.**	**No 6.**	**No 7.**	**No 8.**	**No 9.**	**No 10.**
Concentration (ng/µL)[1]	10.0	5.00	2.50	1.00	0.80	0.50	0.40	0.20	0.10	0.08
Average peak area[2]	1898510	930498	487797	199921	160618	96405	65104	21230	15755	12894
SD	21552	7487	23358	8014	748	2960	11572	2038	1589	1007.
RSD%	*1.13*	*0.80*	*4.78*	*4.00*	*0.46*	*3.07*	*17.77*	*9.60*	*10.08*	*7.81*

[1]WFS1 PCR samples were diluted with dilution buffer. [2]Average peak area was determined from triplicate measurements for each concentration.